High-resolution *KLL* Auger spectra of multiply ionized oxygen projectiles studied by zero-degree electron spectroscopy

R. Bruch,* N. Stolterfoht,† S. Datz, P. D. Miller, P. L. Pepmiller, Y. Yamazaki,‡
H. F. Krause, and J. K. Swenson§
Oak Ridge National Laboratory, Oak Ridge, Tennessee 37831

K. T. Chung and B. F. Davis**
Department of Physics, North Carolina State University, Raleigh, North Carolina 27695
(Received 17 October 1986)

High-resolution measurements of oxygen K Auger electrons have been performed using multiply charged 10-MeV O^{n+} ($n=2$, 3, and 4) projectiles in collisions with He. Line-broadening effects are strongly reduced so that high-resolution spectroscopy is possible for Auger electrons ejected from fast projectiles. The spectra obtained for O^{4+} and O^{3+} impact show relatively simple structures dominated by lines arising from three-electron (Li-like) and four-electron (Be-like) states, respectively. Using configuration-interaction wave functions, the relativistic energies and fine structures of Li-like states are studied. The relativistic correction, Breit-Pauli operator, and mass-polarization effect are calculated for numerous resonances and metastable autoionizing states in O VI. Excellent agreement with experimental data is obtained. For example, the calculated transition energy of the $(1s\,2s\,2p)^4P^\circ$ state is 416.02 eV. It is to be compared with the corresponding experimental data of 416.0±0.2 eV.

I. INTRODUCTION

High-resolution Auger spectroscopy of inner-shell excited highly stripped ions[1,2] is a fascinating tool with tremendous implications for ion-atom collision processes,[3] astrophysics, dynamical behavior of fusion plasmas, lasing media, surfaces, and many-body atomic structure calculations.[4–10] In particular, the effect of relativity has been found to have a pronounced influence on the energy level structure and transition rates associated with Li-, Be-, and B-like core-excited states. Most of the early projectile Auger spectroscopic data,[11] however, was limited by (i) severe kinematic line broadening, (ii) line blending due to overlapping Auger structures, and (iii) cascade repopulation.[12] Recently, Stolterfoht and co-workers[1,13–15] have demonstrated that high-energy resolution, $\Delta E/E \simeq 10^{-3}$, full width at half maximum (FWHM), may be achieved by measuring the projectile electron emission near zero degrees. This resolution is generally sufficient to resolve individual Auger lines. Furthermore, by taking advantage of various kinematic effects[1,14] it should be possible to determine projectile Auger energies within an accuracy of $\sim 10^{-4}$. This improvement is particularly important, since the absolute energy calibration of Auger spectra is difficult in general.[16] Therefore, the zero-degree Auger spectroscopy technique in combination with selective inner-shell ionization (needle ionization) may open new avenues of research for accurate studies of energy levels, widths, branching ratios, and fine-structure splittings of multiply charged core-excited Rydberg ions.

The purpose of this joint experimental and theoretical work is to probe fundamental atomic structure theories. Measurements, for example, of the level structure of highly stripped heavy ions provide important tests of the relativistic many-body problem. As a prototype case, we have studied the formation of Li-, Be-, and B-like singly core-excited oxygen ions produced in collisions of 10-MeV O^{n+} ($n=4$, 3, and 2) projectiles incident on He gas. Theoretically, we have calculated energy values and fine-structure splittings for numerous Li-like states in O VI to high accuracy by means of multiconfiguration-interaction wave functions and by taking relativistic and mass-polarization corrections into account. Excellent agreement is found between our theoretical results and experimental data.

The zero-degree spectroscopy method is described in Sec. II and the experimental K Auger spectra are presented in Sec. III. The theoretical procedure for the calculation of the Li-like states and fine-structure splittings in O VI is outlined in Sec. IV. A comparison of experimental and theoretical results is given in Sec. V. Finally, our new data are summarized in Sec. VI.

II. EXPERIMENTAL TECHNIQUE

The experiments were performed at the Oak Ridge National Laboratory EN-Tandem facility using the zero-degree Auger spectroscopy apparatus[1] temporarily transported from the Hahn-Meitner-Institut, Berlin. The experimental setup is shown schematically in Fig. 1. Electrons produced under single-collision condition were measured at the observation angle of 0° with respect to the beam direction by a tandem electron spectrometer. It consists of two consecutive 90° parallel-plate electrostatic analyzers, where the first one is used to steer the electrons out of the ion beam and the second device determines the

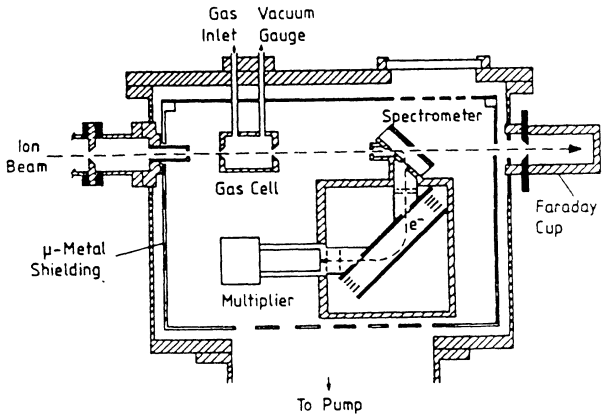

FIG. 1. Experimental setup showing the target-gas cell and tandem-type electron spectrometer.

electron energy resolution. High resolution, of the order of $\Delta E/E \simeq 10^{-3}$, was achieved by deceleration of the electrons between two grids in front of the second analyzer.

Care was taken to maintain single-collision conditions. The target cell has a length of 5 cm. The He gas pressure in the scattering chamber was about 4×10^{-4} Torr when the gas pressure in the target cell was 2×10^{-2} Torr. To ensure a linear pressure dependence of the electron yield, measurements were made for different target-gas pressures. The beam current was typically 100 nA. Generally, count rates of several thousand counts per second were achieved so that a high-resolution electron spectrum could be acquired in a period of about half an hour.

III. OXYGEN *K* AUGER SPECTRA

Figure 2 displays a characteristic electron spectrum measured at 0° observation angle for 10-MeV O^{3+} + He.

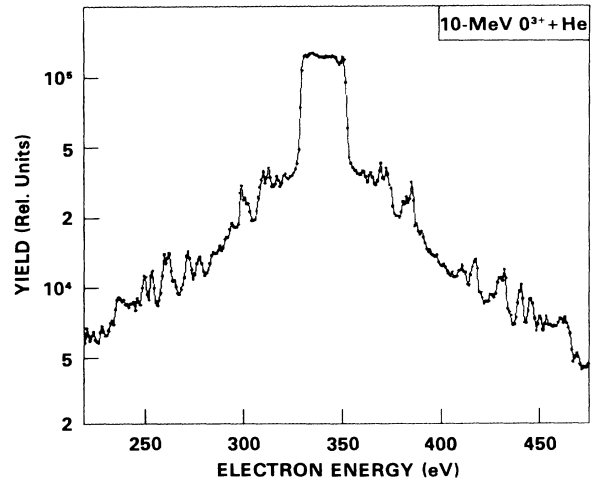

FIG. 2. Low-energy autoionization electrons seen in the vicinity of the electron loss to continuum (ELC). The energy refers to the laboratory rest frame.

The dominating peak (cusp) is due to electron loss to the continuum[17] (ELC), whereas the low- and high-energy lines in the vicinity of the cusp originate from the ejection of projectile autoionization electrons emitted at 180° and 0° in the projectile frame, respectively.

The comparison of the transformed spectra in the source particle frame allows the determination of the reduced projectile energy t_1 as well as the electron energy ε' with relatively high accuracy. For 0° observation angle, we obtain

$$\varepsilon_H = (t_1^{1/2} + \varepsilon'^{1/2})^2 , \tag{1a}$$

$$\varepsilon_L = (t_1^{1/2} - \varepsilon'^{1/2})^2 , \tag{1b}$$

where ε_L and ε_H are energies of corresponding autoionization or Auger lines in the low and high energy range, respectively. In this work we adjusted the projectile energy until the corresponding oxygen autoionization structures coincided in position. This adjustment procedure yielded the unknown projectile energy with an accuracy of about 10^{-4}. Using this value we then determined accurate *K* Auger energies for Li- and Be-like states.

In Fig. 3 high-resolution *K* Auger spectra are shown for (a) 10-MeV O^{4+}, (b) 10-MeV O^{3+}, and (c) 10-MeV O^{2+} incident on He after background subtraction and

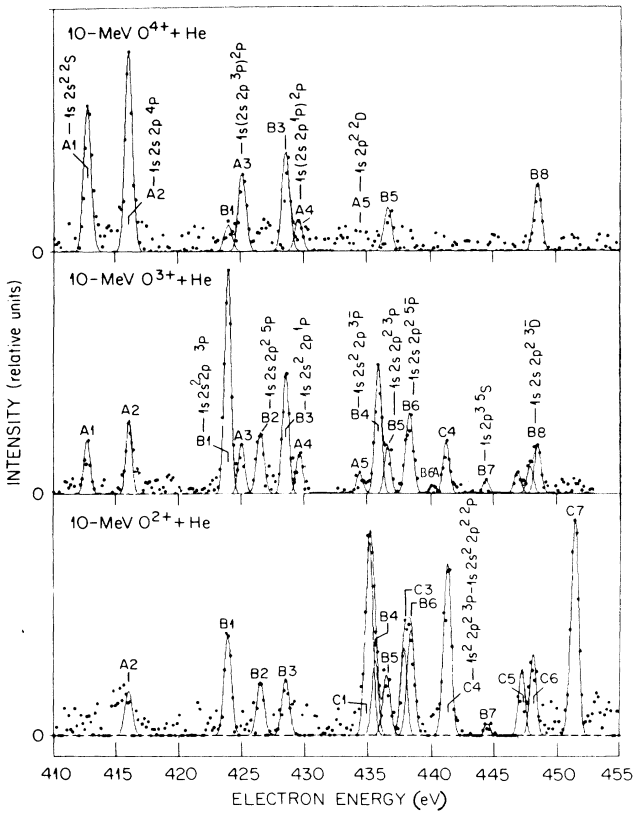

FIG. 3. High-resolution *K* Auger spectra from 10-MeV O^{n+} ($n=4$, 3, and 2) projectiles colliding with He atoms. Background has been subtracted and electron energies have been transformed to the projectile rest frame.

transformation into the projectile rest frame. Most of the prominent Auger peaks were fitted by a Lorentzian curve folded with the Gaussian spectrometer response function. It is important to note that for projectile Auger electrons, whose energies are shifted kinematically to higher values, the contact potentials lose relative importance. When the energies are transformed back to the projectile rest frame, the uncertainty by the contact potentials is reduced by the factor $\sim(\varepsilon'/t_1)^{1/2}$. Hence, for fast collisions ($t_1 \gg \varepsilon'$), a significant reduction of the uncertainty due to contact potentials is achieved.

In this study the uncertainty in the determination of the relative energies is of the order of 0.1 eV. Absolute values are determined with an uncertainty of about ± 0.2 eV. Compared with previous results of Bruch *et al.*[11] the accuracy of the energy determination has been improved by a factor ~ 10. The charge-state dependence of the measured oxygen K Auger structures is discussed in the following.

A. O^{4+} + He

The spectrum obtained for O^{4+} impact on He indicates relatively simple Auger structures dominated by transitions arising from three-electron states. The strongest line in the spectrum labeled $A2$ can be uniquely identified as the $[1s(2s\,2p)^3P^\circ]^4P^\circ$ metastable state. This state may be formed by the removal of a single $1s$ electron from the incident metastable $(1s^2 2s\,2p)^3P^\circ$ state. Furthermore, peak $A3$ is attributed to the decay of $[1s(2s\,2p)^3P^\circ]^2P^\circ$ in O VI. We note that this state is most probably created by "needle ionization" from the $(1s^2 2s\,2p)^3P^\circ$ initial state. Another prominent line labeled $A1$ refers to the $(1s\,2s^2)^2S \rightarrow (1s^2)^1S$ Auger decay. The formation of the $(1s\,2s^2)^2S$ core-excited state can take place via single K-shell ionization from the incident $O^{4+}(1s^2 2s^2)$ ground-state configuration. It is evident from Fig. 3(a) that the formation of the $[1s(2s\,2p)^1P^\circ]^2P^\circ$ ($A4$) and $(1s\,2p^2)^2D$ ($A5$) states is very weak. We note that the relative Auger yields from the $(1s\,2s^2)^2S$, $[1s(2s\,2p)^3P^\circ]^4P^\circ$, and $^2P^\circ$ states directly relate to the original population of the incident $O^{4+}(1s^2 2s^2)^2S$ ground and $O^{4+}(1s^2 2s\,2p)^3P^\circ$ metastable states. From the observed spectrum we have deduced a metastable fraction of the incoming beam of $65\% \pm 5\%$. Finally, we note that the Be-like configurations $1s\,2s^2 2p$ and $1s\,2s\,2p^2$ ($B1$, $B5$, and $B8$) are probably created by a $1s \rightarrow 2p$ dipole excitation process.

B. O^{3+} + He

A striking feature of this spectrum is the weakness of the first two Li-like lines $A1$ and $A2$ when compared to the O^{4+} + He collision system. We therefore conclude that in energetic O^{3+} + He collisions Be-like states are formed most abundantly. In fact, the dominating lines $B1$, $B3$, and $B4$ originate from the $(1s\,2s^2 2p)$ initial configuration created by single ionization of a $1s$ electron from the incident state $1s^2 2s^2 2p$ of O^{3+}. The Auger lines ($B2$, $B5$, $B6$, and $B8$) are attributed to the configuration $1s\,2s\,2p^2$ formed by the ionization of a $1s$ electron from the initial metastable state $(1s^2 2s\,2p^2)^4P$ of O^{3+}. From the relative line intensities we estimated the fraction of metastable $O^{3+}(1s^2 2s\,2p^2)^4P$ states to be about 55% when compared to the $O^{3+}(1s^2 2s^2 2p)^2P^\circ$ plus metastable state composition. In particular, the population of the metastable $(1s\,2s\,2p^2)^5P$ state may arise via single K-shell ionization from $(1s^2 2s\,2p^2)^4P$. We also conclude that there is no clear indication of B-like lines except peak $C4$ which we tentatively assign as being due to the decay of the $1s\,2s^2 2p^2$ initial configuration.

C. O^{2+} + He

Most of the Auger lines observed above 430 eV [see Fig. 3(c)] originate from B-like initial configurations. Due to a lack of accurate theoretical transition energies and branching ratios, a unique line identification of each line structure is difficult so far. However, the line assignment may be simplified by assuming that the configuration $1s\,2s^2 2p^2$ is predominantly produced. It may be formed via ionization of a single $1s$ electron in accordance with the results for O^{3+} and O^{4+} ion impact on He. If we further assume a specific fraction of metastable $(1s^2 2s\,2p^3)^5S^\circ$ O^{2+} ions in the incoming beam, then $1s\,2s\,2p^3$ configurations should also be populated in the O^{2+} + He collision processes. In particular, the metastable autoionizing $O^{3+}(1s\,2s\,2p^3)^6S^\circ$ states may be formed.

IV. THEORETICAL CALCULATIONS FOR Li-LIKE STATES IN O VI

In order to test electron correlation and relativistic interactions in Li-like oxygen, we have performed detailed theoretical studies of the Auger line energies and fine-structure splittings of numerous core-excited states in O VI. The energy values are presented in Table I and the fine-structure splittings for the doublet and quartet states of O VI are listed in Tables II and III, respectively.

The method for the computation of the energy levels and wave functions of the Coulombic autoionizing states with angular and spin symmetry ^2S, $^2P^\circ$, and ^2D is the same as that of Davis and Chung.[19] For these states the saddle-point technique is used which builds a $1s$ vacancy in the wave function. To achieve convergence for the nonrelativistic energy, we have used anywhere from 13 to 16 angular and spin partial waves and 97—110 linear parameters. The quartet states and the doublet states with angular and spin symmetry ^2P, $^2D^\circ$, and ^2F are metastable against autoionization in the nonrelativistic limit by conservation of parity and spin; therefore, these states may be computed with the standard Rayleigh-Ritz variation method. The trial wave function and procedure for implementing the Rayleigh-Ritz variation method for the doublet states of O VI calculated here is the same as that of Ref. 19 and for the quartet states the corresponding calculation is described in Chung and Davis.[21] The nonrelativistic energies for these doublet and quartet states were obtained with anywhere from 6 to 15 angular and spin partial waves and 43—110 linear parameters.

The results for the nonrelativistic energies are given in Table I. The configuration designations of these states are based on an examination of the relative magnitudes of the normalization integrals of the individual partial waves. Also given in this table is the total relativistic correction

TABLE I. Energies for numerous core-excited states in O VI. E_{nr} is the nonrelativistic energy, C is the first-order relativistic and mass-polarization corrections, $E_{tot}=E_{nr}+C$, E_{auger} is the energy of the auger electron; computed using the ground-state energy for O VII, −59.198 24 a.u. (Ref. 18): this result includes relativistic and mass polarization corrections, and the rydberg appropriate for oxygen, 13.605 336 1 eV.

State	E_{nr} (a.u.)	C (a.u.)	E_{tot} (a.u.)	E_{auger} (eV)
$(1s\,2p\,2p)^2P$	−43.136 297	−0.031 342	−43.167 621	436.20
$((1s\,2p)^3P,3p)^2P$	−40.431 640	−0.030 072	−40.461 712	509.83
$((1s\,2p)^1P,3p)^2P$	−40.190 567	−0.030 369	−40.220 935	516.39
$((1s\,2p)^3P,3d)^2D^\circ$	−40.347 918	−0.029 453	−40.377 370	512.13
$((1s\,2p)^1P,3d)^2D^\circ$	−40.123 405	−0.029 951	−40.153 356	518.22
$((1s\,2p)^3P,4d)^2D^\circ$	−39.423 644	−0.029 362	−39.453 005	537.28
$((1s\,2p)^3P,4f)^2F$	−39.404 490	−0.029 327	−39.433 817	537.80
$((1s\,2p)^3P,5f)^2F$	−38.994 471	−0.029 316	−39.023 786	548.96
$((1s\,2p)^3P,6f)^2F$	−38.772 203	−0.029 315	−38.801 518	555.01
$(1s\,2s\,3s)^4S$	−40.867 311	−0.035 390	−40.902 701	497.83
$(1s\,2p\,3p)^4S$	−40.398 457	−0.030 330	−40.428 787	510.73
$(1s\,2s\,4s)^4S$	−39.790 837	−0.034 461	−39.825 298	527.15
$(1s\,2s\,2p)^4P^\circ$	−43.874 513	−0.035 016	−43.909 529	416.02
$(1s\,2s\,3p)^4P^\circ$	−40.722 225	−0.034 203	−40.756 428	501.81
$(1s\,2p\,3s)^4P^\circ$	−40.527 949	−0.030 998	−40.558 947	507.19
$(1s\,2p\,2p)^4P$	−43.396 832	−0.030 641	−43.427 473	429.13
$(1s\,2p\,3p)^4P$	−40.382 579	−0.029 869	−40.412 448	511.17
$(1s\,2p\,4p)^4P$	−39.442 174	−0.029 560	−39.471 734	536.77
$(1s\,2s\,3d)^4D$	−40.633 133	−0.033 593	−40.666 726	504.25
$(1s\,2p\,3p)^4D$	−40.440 178	−0.030 260	−40.470 438	509.60
$(1s\,2s\,4d)^4D$	−39.700 548	−0.033 932	−39.734 480	529.62
$(1s\,2p\,3d)^4D^\circ$	−40.304 468	−0.029 452	−40.333 920	513.31
$(1s\,2p\,3d)^4F^\circ$	−40.364 316	−0.029 499	−40.393 815	511.68
$(1s\,2p\,5g)^4G^\circ$	−38.991 696	−0.029 316	−39.021 012	549.04
$(1s\,2s\,2s)^2S$	−43.996 514	−0.037 637	−44.034 151	412.63
$(1s\,2p\,2p)^2S$	−42.879 574	−0.031 266	−42.910 839	443.19
$((1s\,2s)^3S,3s)^2S$	−40.764 555	−0.034 816	−40.799 371	500.65
$(1s\,(2s\,2p)^3P)^2P^\circ$	−43.545 176	−0.034 436	−43.579 612	424.99
$(1s\,(2s\,2p)^1P)^2P^\circ$	−43.372 542	−0.033 859	−43.406 400	429.71
$((1s\,2s)^3S,3p)^2P^\circ$	−40.710 530	−0.033 898	−40.744 428	502.14
$(1s\,2p\,2p)^2D$	−43.203 794	−0.031 000	−43.234 794	434.38
$((1s\,2s)^3S,3d)^2D$	−40.576 891	−0.033 798	−40.610 689	505.78

for each state. These results were obtained from first-order perturbation theory and include relativistic correction to the kinetic energy, Darwin term, and retardation effect or orbit-orbit term. The mass-polarization effect, which is a nonrelativistic correction, is also computed in first-order perturbation theory; its contribution is included in the relativistic correction. For a discussion of the procedure for computing the relativistic and mass-polarization effects, the reader is referred to Ref. 21. For a discussion of the relative magnitudes of the individual contributions of each perturbation operator, the reader is referred to the analyses of these effects for the lower-Z three-electron ions considered in Refs. 19 and 21–23.

The splittings of the multiplets are computed by first forming eigenfunctions of total angular momentum J. With these eigenfunctions the first-order perturbations due to the spin-orbit, spin-other-orbit, and spin-spin effects are evaluated. The details of this calculation are described in Ref. 21. The results of the calculations performed here for the doublet and quartet states of O VI are given in Tables II and III, respectively.

V. COMPARISON OF EXPERIMENTAL AND THEORETICAL RESULTS

Table IV compares the Auger energies resulting from either the Coulombic or spin-induced autoionization of the states given in Table I with experiment and other theory. In Table IV both the relativistic and the nonrelativistic energies are quoted relative to the relativistic ground-state energy of Pekeris,[18] −59.198 24 a.u. The Auger energies are given in electron volts, where the conversion 27.210 672 2 eV/a.u. was used. The uncertainties of the relative Auger energies originating from $(1s\,2s^2)^2S$, $(1s\,2s\,2p)^4P^\circ$, $[1s\,(2s\,2p)^3P]^2P^\circ$, and $[1s\,(2s\,2p)^1P]^2P^\circ$ are of the order of 0.2 eV corresponding to an accuracy $\Delta E/E$ of about 2×10^{-4} (0.02%). The calculated and experimentally determined energy positions coincide extremely well.

We therefore conclude that the theoretical method used in this work is very well suited to generate very accurate resonance energies for singly core-excited states of the Li-isoelectronic series, in particular for the lower-Z elements.

TABLE II. Fine structures for the doublet states of O VI. L is the total orbital angular momentum of the state; $\langle C_{SO} \rangle$ and $\langle C_{SOO} \rangle$ are reduced matrix elements for the spin-orbit and spin-other-orbit interactions, respectively (see Refs. 19 and 20).

State	$\langle C_{SO} \rangle$ 10^4 (a.u.)	$\langle C_{SOO} \rangle$ 10^4 (a.u.)	$[E(L+0.5)-E(L-0.5)]$ (cm^{-1})
$(1s\,2p\,2p)^2P$	9.8025	−0.4696	614.5
$((1s\,2p)^3P,3p)^2P$	2.6262	−2.5534	4.79
$((1s\,2p)^1P,3p)^2P$	4.3860	−0.4011	262.4
$((1s\,2p)^3P,3d)^2D^\circ$	1.3684	−0.1060	138.5
$((1s\,2p)^1P,3d)^2D^\circ$	0.9112	0.0024	100.3
$((1s\,2p)^3P,4d)^2D^\circ$	1.7171	−0.1561	171.3
$((1s\,2p)^3P,4f)^2F$	0.9426	−0.1077	128.3
$((1s\,2p)^3P,5f)^2F$	0.9563	−0.0989	131.7
$((1s\,2p)^3P,6f)^2F$	0.9648	−0.1442	126.1
$(1s(2s\,2p)^3P)^2P^\circ$	5.7736	−0.1512	370.2
$(1s(2s\,2p)^1P)^2P^\circ$	4.6498	−4.0858	37.1
$((1s\,2s)^3S,3p)^2P^\circ$	−0.5107	−0.9930	−99.0
$(1s\,2p\,2p)^2D$	0.6622	−3.4815	−309.4
$((1s\,2s)^3S,3d)^2D$	−0.0281	−0.0151	−4.74

On the other hand, nonrelativistic calculations are generally inadequate to predict the experimental line positions correctly.

We have also extracted Auger line energies for the most prominent Be-like states. These experimental values are listed in Table V along with existing theoretical predictions and previous experimental results. The line identification is mainly based on the work of Bruch *et al.*[11] We have also included in this table recent theoretical results of Chen who has applied the multiconfiguration Dirac-Fock (MCDF) method taking the generalized Breit interaction and quantum-electrodynamic corrections into account.[6] The apparent discrepancies between theory and experiment for transition energies are probably due to the inadequacy in the calculations of correlation corrections using a limited configuration-interaction approach. Generally better agreement is found for the *ab initio* calculations of Bruch *et al.*[11] which are based on the generalized Brillouin theorem (GBT) multiconfiguration (MC) method. In this case the calculated energies were semiempirically corrected for external correlation and relativistic energy contributions.

For the O^{3+} + He collision system [see Fig. 3(b) and Table V] the most intense line structures can be assigned to Be-like initial states. Thus the most prominent peak ($B1$) centered at 423.9±0.2 eV is uniquely identified as the $(1s2s^22p)^3P^\circ \rightarrow (1s^22p\varepsilon s)^3P^\circ$ transition in O V. Another pronounced line ($B4$) at 435.9±0.2 eV arises from the competing $(1s2s^22p)^3P^\circ \rightarrow (1s^22s\varepsilon p)^3P^\circ$ Auger decay. A remarkable feature seen from Fig. 3(b) is that the $B6A$ $(1s2s^22p)^1P^\circ \rightarrow (1s^22s\varepsilon p)^1P^\circ$ transition is very weak compared to the dominating $(1s2s^22p)^1P^\circ \rightarrow (1s2p\varepsilon s)^1P^\circ$ one

TABLE III. Fine structures for the quartet states of O VI. L is the total orbital angular momentum of the state; $\langle C_{SO} \rangle$, $\langle C_{SOO} \rangle$, and $\langle C_{SS} \rangle$ are reduced matrix elements for the spin-orbit, spin-other-orbit, and spin-spin interactions, respectively (see Refs. 19 and 20). $J=L+1.5$, $J_1=L+0.5$, $J_2=L-0.5$, $J_3=L-1.5$, where J is the total angular momentum.

State	$\langle C_{SO} \rangle$ 10^4 (a.u.)	$\langle C_{SOO} \rangle$ 10^4 (a.u.)	$\langle C_{SS} \rangle$ 10^6 (a.u.)	$(E_J-E_{J_1})$ (cm^{-1})	$(E_{J_1}-E_{J_2})$ (cm^{-1})	$(E_{J_2}-E_{J_3})$ (cm^{-1})
$(1s\,2s\,2p)^4P^\circ$	5.2079	−2.0898	9.0495	401.7	98.0	
$(1s\,2s\,3p)^4P^\circ$	1.3500	−0.5253	2.2712	105.5	27.4	
$(1s\,2p\,3s)^4P^\circ$	5.5108	−2.1311	8.5804	427.4	120.8	
$(1s\,2p\,2p)^4P$	5.1773	−2.3595	−9.0715	249.5	293.0	
$(1s\,2p\,3p)^4P$	3.4842	−1.4630	−5.6314	184.7	199.8	
$(1s\,2p\,4p)^4P$	3.1590	−1.2607	−4.8893	176.1	182.9	
$(1s\,2s\,3d)^4D$	0.4631	−0.2161	0.3089	46.5	21.0	7.74
$(1s\,2p\,3p)^4D$	3.3098	−1.2888	1.6700	356.7	188.8	86.9
$(1s\,2s\,4d)^4D$	0.1140	−0.0495	0.0874	12.3	5.35	1.83
$(1s\,2p\,3d)^4D^\circ$	1.1352	−0.4675	−1.4253	63.2	101.4	83.4
$(1s\,2p\,3d)^4F^\circ$	2.0168	−0.8258	0.6436	273.4	165.2	92.5
$(1s\,2p\,5g)^4G^\circ$	0.2981	−0.1165	−0.4346	−0.234	51.3	72.0

(B 3). From the observed spectra branching ratios for the $^1P^\circ$ and $^3P^\circ$, terms have been determined which can be used to test electron correlation and interchannel coupling in four-electron systems. The striking difference of the branching ratios associated with the $(1s\,2s^2 2p)^3P^\circ$ and $^1P^\circ$ states will be discussed in detail elsewhere.[28,29]

Another interesting result is the strong population of the Be-like metastable autoionizing $(1s\,2s\,2p^2)^5P$ term which decays to the $1s^2 2p$ and $1s^2 2s$ final ionic states, giving rise to two peaks appearing at 426.5 ± 0.2 and 438.55 ± 0.2 eV, respectively. Such high spin states in connection with single-collision excitation have been observed earlier by Bruch *et al.*[11,30] and Schneider *et al.*[11] Recently, Berry and co-workers[31] have measured the

TABLE IV. Comparison between predicted and experimental Auger transition energies (in eV) originating from core-excited states in O VI.

	Nonrelativistic		Relativistic		Experiment	
State	This work	Other theory	This work	Other theory	This work	Other groups
$(1s\,2s\,2s)^2S$	413.65		412.63	412.6[a]	412.7±0.2	
$(1s\,2s\,2p)^4P^\circ$	416.97	418.18[b]	416.02	417.3[b]	416.0±0.2	416.0±1.0[c]
		417.31[d]				
		417.12[e]				
$(1s(2s\,2p)^3P)^2P^\circ$	425.93	426.62[d]	424.99		425.0±0.2	
$(1s\,2p\,2p)^4P$	429.97	430.32[b]	429.13	429.5[b]		429.1±1.0[c]
		430.44[d]		428.29[f]		
		430.12[e]				
$(1s(2s\,2p)^1P)^2P^\circ$	430.63	432.67[d]	429.71		429.6±0.2	
$(1s\,2p\,2p)^2D$	435.22	436.92[d]	434.38	434.66[f]	434.4±0.2	
				434.4[a]		
$(1s\,2p\,2p)^2P$	437.06	437.39[b]	436.21	436.6[b]		
		438.29[d]		436.04[f]		
$(1s\,2p\,2p)^2S$	444.04	442.72[d]	443.19	443.96[f]		
				443.2[a]		
$(1s\,2s\,3s)^4S$	498.80	501.12[b]	497.83	500.2[b]		
		498.92[e]				
$(1s\,2s\,3p)^4P^\circ$	502.74	504.74[b]	501.81	503.9[b]		
		503.20[e]				
$(1s\,2s\,3d)^4D$	505.17		504.25	505.8[b]		
$(1s\,2p\,3s)^4P^\circ$	508.03	509.04[b]	507.19	508.2[b]		
		508.92[e]				
$(1s\,2p\,3p)^4D$	510.42		509.60	510.0[b]		
$((1s\,2p)^3P,3p)^2P$	510.65	510.97[b]	509.83	510.2[b]		
$(1s\,2p\,3p)^4S$	511.55	512.00[b]	510.73	511.1[b]		
		512.33[e]				
$(1s\,2p\,3p)^4P$	511.99	512.33[b]	511.17	511.5[b]		
		512.14[e]				
$(1s\,2p\,3d)^4F^\circ$	512.48		511.68	511.8[b]		
$((1s\,2p)^3P,3d)^2D^\circ$	512.93		512.13	512.3[b]		
$(1s\,2p\,3d)^4D^\circ$	514.11		513.31	513.5[b]		
$((1s\,2p)^1P,3p)^2P$	517.21	517.53[b]	516.39	516.8[b]		
$((1s\,2p)^1P,3d)^2D^\circ$	519.04		518.22	518.4[b]		
$(1s\,2s\,4s)^4S$	528.09	530.75[b]	527.15	529.9[b]		
		528.52[e]				
$(1s\,2s\,4d)^4D$	530.55		529.62	531.8[b]		
$(1s\,2p\,4p)^4P$	537.58	537.83[b]	536.77	537.1[b]		
		540.42[e]				
$((1s\,2p)^3P,4d)^2D^\circ$	538.08		537.28	537.4[b]		

[a]S. Goldsmith (Ref. 27) and R. Bruch, D. Schneider, W. H. E. Schwarz, M. Meinhart, B. M. Johnson, and K. Taulbjerg (Ref. 11).
[b]B. R. Junker and J. N. Bardsley (Ref. 24). For their relativistic Auger energy they use an estimated relativistic effect for the metastable state and an experimental energy of -59.198 a.u. for the $(1s\,1s)^1S$ target state.
[c]R. Bruch, D. Schneider, W. H. E. Schwarz, M. Meinhart, B. M. Johnson, and K. Taulbjerg (Ref. 11).
[d]J. Hata and I. P. Grant (Ref. 25). Nonrelativistic terms were obtained by taking the nonrelativistic limit ($C=137\times10^4$ a.u.) in a MCDF-OL calculation.
[e]E. Holøien and S. Geltman (Ref. 26).
[f]M. H. Chen, B. Crasemann, and H. Mark (Ref. 5).

TABLE V. Comparison between some predicted and experimental Auger transition energies (in eV) associated with core-excited states in O V.

Initial state	Final ionic state	theory		Experiment: This work	Experiment: Other groups
$(1s\,2s^2\,2p)^3P^\circ$	$1s^2\,2p$	424.2[a] 424.54[b]	$B1$	423.9±0.2	424±1.0[a]
$(1s\,2s\,2p^2)^5P$	$1s^2\,2p$	426.7[a] 426.22[b]	$B2$	426.5±0.2	426.2±1.0[a]
$(1s\,2s^2\,2p)^1P^\circ$	$1s^2\,2p$	428.5[a] 429.07[b]	$B3$	428.5±0.2	428±1.0[a]
$(1s\,2s^2\,2p)^3P^\circ$	$1s^2\,2s$	436.2[a] 436.63[b]	$B4$	435.9±0.2	
$(1s\,2s\,2p^2)^3P$	$1s^2\,2p$	436.4[a]	$B5$	436.6±0.2	
$(1s\,2s\,2p^2)^5P$	$1s^2\,2s$	438.7[a] 438.33[b]	$B6$	438.55±0.2	438.2±1.0[a]
$(1s\,2s^2\,2p)^1P^\circ$	$1s^2\,2s$	440.5[a] 441.16[b]	$B6A$	440.5±0.2	440±2.0[a]
$(1s\,2p^3)^5S$	$1s^2\,2p$	444.35[a] 444.18[b]	$B7$	444.4±0.2	

[a]R. Bruch, D. Schneider, W. H. E. Schwarz, M. Meinhart, B. M. Johnson, and K. Taulbjerg (Ref. 11).
[b]M. H. Chen (Ref. 6).

wavelength of the $(1s\,2s\,2p^2)^5P \rightarrow (1s\,2p^3)^5S^\circ$ optical transition in O V using the beam-foil technique. In fact, a small line appearing at 444.4 eV [see Fig. 3(b)] may be attributed to the $(1s\,2p^3)^5S^\circ \rightarrow (1s^2\,2p)^2P^\circ$ time-delayed Auger decay. This assignment is supported by the recent calculation of the Auger and x-ray transition rates for states of the $1s\,2p^3$ configuration of Be-like ions.[6] In particular, for O^{4+} 34.8% of the initial $(1s\,2p^3)^5S_2$ states should decay by electron emission whereas 65.2% are depleted by photon emission. For even higher atomic numbers ($Z > 8$) the Auger decay channel is expected to dominate over optical emission.

Finally, we note that the line identification and quantitative analysis of the O^{2+} + He spectrum, displayed in Fig. 3(c), is difficult due to the lack of accurate theoretical calculations. In addition, the assignment is complicated by the increasing number of Auger decay channels in B- and C-like ions. For example, B-like states arising from the $(1s\,2p^3)$ configuration can in general decay to the $(1s^2\,2s\,2p)^3P^\circ$ and $^1P^\circ$, $(1s^2\,2p^2)^3P$, ^1D, and ^1S final ionic states.

VI. CONCLUSIONS

In conclusion, the method of zero-degree Auger spectroscopy has been applied to study the level structure and relative intensities of multiply charged oxygen ions. These measurements provide important tests of the multielectron relativistic and quantum electrodynamic effects. It has been shown that these corrections are of the order of 1 eV for $Z = 8$ and cannot be neglected. We have also demonstrated that high energy resolution comparable to optical emission studies[10,32,33] can be achieved by taking advantage of the reduction of kinematic line-broadening effects and the transformation of the Auger spectra from the laboratory to the projectile rest frame.[13] Such high resolution in the region of multiply excited and ionized few-electron systems opens a wide field of accurate measurements of energy levels, fine-structure splittings, branching ratios, and Auger widths as a function of the atomic number Z.[16]

ACKNOWLEDGMENTS

Research for this work was sponsored by the U.S. Department of Energy, Division of Basic Sciences, under Contract No. DE-AC05OR21400 with Martin Marietta Energy Systems, Inc. and Research Corporation (R.B.). This work is supported by the National Science Foundation, Grant No. PHY-84-05649 (K.T.C., B.F.D.). This research was also supported by a grant from Research Corporation (B.F.D.). R. Bruch is indebted to Dr. Chen from the Lawrence Livermore National Laboratory for the communication of unpublished data.

*Also at Department of Physics, University of Nevada, Reno, Reno, NV 89557.
†Also at Hahn-Meitner Institut für Kernforschung, Berlin GmBH, West Germany.
‡Also at Research Laboratory for Nuclear Reactors, Tokyo Institute of Technology, Japan.
§Also at Department of Physics, University of North Carolina, Chapel Hill, NC 27514.
**Also at Dept. of Physics, University of North Carolina at Wilmington, Wilmington, NC 28403.

[1]N. Stolterfoht, Phys. Rep. **146**, 315 (1987), and references quoted therein.
[2]D. Schneider, N. Stolterfoht, A. Itoh, T. Schneider, G. Schiwietz, W. Zeitz, and T. Zouros, *Electronic and Atomic Collisions,* edited by D. C. Lorentz, W. E. Meyerhof, and I. R. Peterson (Elsevier, Amsterdam, 1986), p. 671.
[3]S. Datz, *Atomic Physics,* edited by I. Lindgren, A. Rosen, and S. Svanberg (Plenum, New York, 1983), Vol. 8, p. 369.
[4]M. H. Chen, B. Crasemann, and H. Mark. Phys. Rev. A **24**, 1852 (1981).
[5]M. H. Chen, B. Crasemann, and H. Mark. Phys. Rev. A **26**, 1441 (1982).
[6]M. H. Chen, Phys. Rev. A **31**, 1449 (1985).
[7]K. T. Chung, Phys. Rev. A **29**, 682 (1984).
[8]K. T. Chung, and R. Bruch, Phys. Rev. A **28**, 1418 (1983).
[9]R. Bruch, K. T. Chung, W. L. Luken, and J. C. Culberson, Phys. Rev. A **31**, 310 (1985).
[10]R. Bruch, K. T. Chung, E. Träbert, P. H. Heckmann, B. Raith, and H. R. Müller, J. Phys. B **17**, 333 (1984).
[11]R. Bruch, D. Schneider, W. H. E. Schwarz, M. Meinhart, B. M. Johnson, and K. Taulbjerg, Phys. Rev. A **19**, 587 (1979).
[12]D. Schneider, R. Bruch, W. Butscher, and W. H. E. Schwarz, Phys. Rev. A **24**, 1223 (1981).
[13]A. Itoh, T. Schneider, G. Schiwietz, Z. Roller, H. Platten, G. Nolte, D. Schneider, and N. Stolterfoht, J. Phys. B **16**, 3965 (1983).
[14]N. Stolterfoht, A. Itoh, D. Schneider, T. Schneider, G. Schiwietz, H. Platten, G. Nolte, R. Glodde, U. Stettner, W. Zeitz, and T. Zouros, in International Conference on X-Ray and Inner Shell Processes in Atoms, Molecules and Solids, Leipzig, German Democratic Republic, 1984 (unpublished).
[15]A. Itoh, D. Schneider, T. J. M. Zouros, G. Nolte, G. Schiwietz, W. Zeitz, and N. Stolterfoht, Phys. Rev. A **31**, 684 (1985).
[16]M. Rødbro, R. Bruch, and P. Bisgaard, J. Phys. B **15**, 2413 (1979).
[17]J. Burgdörfer, M. Breinig, S. B. Elston, and I. A. Sellin, Phys. Rev. A **28**, 3277 (1983).
[18]C. L. Pekeris, Phys. Rev. **112**, 1649 (1958).
[19]B. F. Davis and K. T. Chung, Phys. Rev. A **29**, 2586 (1984).
[20]A. Messiah, *Quantum Mechanics* (Wiley, New York, 1961), Vol. II.
[21]K. T. Chung and B. F. Davis, Phys. Rev. A **29**, 1871 (1984).
[22]K. T. Chung, Phys. Rev. A **29**, 682 (1984).
[23]M. Agentoft, T. Anderson, K. T. Chung, and B. F. Davis, Phys. Scr. **31**, 74 (1985).
[24]B. R. Junker and J. N. Bardsley, Phys. Rev. A **8**, 1345 (1973).
[25]J. Hata and I. P. Grant, J. Phys. B **16**, 915 (1983).
[26]E. Holøien and S. Geltman, Phys. Rev. **153**, 81 (1967).
[27]S. Goldsmith, J. Phys. B **7**, 2315 (1974).
[28]R. Bruch, S. Datz, P. D. Miller, P. L. Pepmiller, H. F. Krause, and N. Stolterfoht, Phys. Rev. A (to be published).
[29]C. A. Nicolaides and T. Mercouris, Phys. Rev. A (to be published).
[30]R. Bruch, M. Rødbro, P. Bisgaard, and P. Dahl, Phys. Rev. Lett. **39**, 801 (1977).
[31]H. G. Berry, R. L. Brooks, K. T. Cheng, J. E. Hardis, and W. Ray, Phys. Scr. **25**, 391 (1982).
[32]T. Anderson and S. Mannervik, Comments At. Mol. Phys. **16**, 185 (1985).
[33]C. Nicolaides and G. Aspromallis, J. Phys. B **16**, L251 (1983).